



Dynamic parameterization of soil surface characteristics for hydrological models in agricultural catchments

Thomas Grangeon, Rosalie Vandromme, Lai Ting Pak, Philippe Martin, Olivier Cerdan, Jean-Baptiste Richet, Olivier Evrard, Véronique Souchère, Anne-Véronique Auzet, Bruno Ludwig, et al.

► To cite this version:

Thomas Grangeon, Rosalie Vandromme, Lai Ting Pak, Philippe Martin, Olivier Cerdan, et al.. Dynamic parameterization of soil surface characteristics for hydrological models in agricultural catchments. CATENA, 2022, 214, pp.106257. 10.1016/j.catena.2022.106257 . hal-03645062

HAL Id: hal-03645062

<https://hal.inrae.fr/hal-03645062>

Submitted on 19 Apr 2022

HAL is a multi-disciplinary open access archive for the deposit and dissemination of scientific research documents, whether they are published or not. The documents may come from teaching and research institutions in France or abroad, or from public or private research centers.

L'archive ouverte pluridisciplinaire **HAL**, est destinée au dépôt et à la diffusion de documents scientifiques de niveau recherche, publiés ou non, émanant des établissements d'enseignement et de recherche français ou étrangers, des laboratoires publics ou privés.

Copyright

1 Dynamic parameterization of soil surface characteristics for
2 hydrological models in agricultural catchments

3 Thomas Grangeon^(a), Rosalie Vandromme^(a), Lai Ting Pak^{(b), (c)}, Philippe Martin^(d), Olivier Cerdan^(a), Jean-
4 Baptiste Richet^(c), Olivier Evrard^(e), Véronique Souchère^(f), Anne-Véronique Auzet^(g), Bruno Ludwig^(h),
5 Jean-François Ouvry^(c)

6 (a) BRGM, F-45060, 45060 Orléans, France

7 (b) UPR HortSys, Cirad, F-97285 Le Lamentin, Martinique, France

8 (c) Association de recherche sur le Ruissellement, l'Erosion et l'Aménagement du Sol (AREAS), 2 Avenue Foch,
9 76460 Saint-Valéry-en-Caux

10 (d) Université Paris-Saclay, INRAE, AgroParisTech, UMR SADAPT, 75005, Paris, France

11 (e) Laboratoire des Sciences du Climat et de l'Environnement (LSCE-IPSL), UMR 8212 (CEA/CNRS/UVSQ),
12 Université Paris-Saclay, Gif-sur-Yvette, France

13 (f) UMR SADAPT, INRAE, AgroParisTech, Université Paris-Saclay, Avenue Lucien Brétignières, 78850 Thiverval-
14 Grignon, France

15 (g) Université de Strasbourg, ITES UMR 7063, Strasbourg F-67084, France

16 (h) LIOSE, 71 Rue de Crécy, 02000 Laon

17 * Corresponding author: t.grangeon@brgm.fr

Abstract

The detrimental impacts of surface runoff and soil erosion, particularly in cultivated areas, call for the use of distributed runoff and soil erosion models with a view to supporting adapted catchment management strategies. However, runoff model parameterization remains challenging in agricultural catchments due to the high spatial and seasonal variability of soil properties. Data acquisition is demanding and may not always be feasible. Therefore, model parameterization in such environments have been the subject of numerous research efforts. The combined analysis of land use management and soil surface state was proposed in literature to address this issue and demonstrated its potential for runoff analysis and modelling. However, these research findings were related to specific rainfall sequences and/or soil surface state. In this study, existing knowledge on soil surface state and its application to runoff model parameterization were synthetized and included in an easy-to-use parameterization software (PREMACHE), providing a framework for modelers lacking of means and/or data for modelling complex agricultural catchments.

To develop and evaluate the software, a dataset was acquired over 9 years on more than 110 plots in a 1045 ha agricultural catchment, including crop types, soil surface state, rainfall and runoff time series. Soil surface state dynamics was modeled based on crop types and daily rainfall. It was evaluated in the experimental catchment and validated in a nearby catchment. Soil hydrodynamic properties (e.g. infiltration capacity) were deduced from this framework and literature data at a daily time step, for each plots. Moreover, runoff events were measured when the modeled infiltration capacity was low, indicating that the parametrization adequately captured its temporal dynamics. The software developed in this study, as well as setup values deduced from the monitoring campaigns are provided with the manuscript for application in other ungauged catchments and explore their impact on agricultural catchment hydrological dynamics.

Keywords: Crops, Soil properties, Runoff, Agricultural catchment, Model parameterization, Soil infiltration capacity, Tillage operations

43 Highlights

- 44 • Parameterization of runoff models is challenging in agricultural catchments
- 45 • Knowledge on using soil surface state for model parameterization was synthesized
- 46 • A comprehensive field survey was performed on a 1045 ha agricultural catchment
- 47 • A simple framework for soil surface state is proposed and evaluated for common crops
- 48 • A software is provided to derive runoff model inputs from rainfall and crop types

49

1. Introduction

Soil erosion may generate numerous detrimental environmental impacts, including the on-site loss of fertile soil and the off-site triggering of muddy floods, resulting in the degradation of the road network and housing (Boardman et al., 1994; Boardman, 2020). Downstream, the increased fine particles load to rivers is detrimental to aquatic environment (Owens et al., 2005). Muddy floods are regularly observed in the European loess belt (Evrard et al., 2007; Boardman, 2010; Evrard et al., 2010), where the soil erodibility is high and agriculture provides the dominant land use (Cerdan et al., 2004). Models are therefore needed to design effective mitigation strategies to reduce erosion and muddy flood impacts. However, the adequate modelling of runoff and erosion in agricultural catchments requires a spatially-distributed description of the highly variable hydrodynamic properties of soil surface (Gascuel-Oudou et al., 2011; Gumiere et al., 2011). Indeed, soil hydrodynamic properties such as infiltration capacities can exhibit large spatial variations, resulting from crop allocation decisions and management operations (Shore et al., 2013), as well as large temporal variations because of crusting and roughness evolution throughout the year.

Different modelling approaches have been applied to agricultural catchments, such as the spatially distributed LISEM (De Roo et al., 1996) or STREAM (Cerdan et al., 2002a; Evrard et al., 2009) models, or the widely used lumped SWAT/SWAT+ model (Arnold et al., 1998; Bieger et al., 2017). In runoff and erosion models, the parameterization used to calculate the partition of rainfall between runoff and infiltration is critical and, as such, questioned (Qi et al., 2020). The curve number approach (Ponce & Hawkins, 1996) has been used in several models, including SWAT. This approach was criticized as being an empirical formulation of runoff, which may result in an incorrect representation of hydrology (Garen and Moore, 2005; Hawkins, 2014). However, using curve number adaptations following methods such as that proposed by Martin et al. (2009) could provide an adequate formulation of infiltration and runoff calculation in agricultural environments. Finding alternative approaches to include the seasonal variability associated with the crop growth and management in these modelling approaches conducted

at the catchment scale remains a topic of wide scientific interest (Nkwasa et al., 2020; Msigwa et al., *under review*).

Another common approach included in hydrological models to describe runoff dynamics is the use of infiltration capacity maps, which can be used to calculate the runoff and infiltration partition using e.g. the Green-Ampt formula (King et al., 1999). Measuring infiltration capacity on multiple plots during the entire crop growth and harvest period and during intercrops, which have a strong impact on runoff and erosion (Cerdan et al., 2002b), would however be time- and labor-consuming and limit their widespread application. To overcome this challenge, many experiments such as those referenced in Cerdan et al. (2002a) were performed to monitor runoff from the plot to the catchment scales in both agricultural and natural environments. These experiments demonstrated that soil surface state, particularly soil crusting, but also soil roughness and crop cover mainly controlled runoff and erosion dynamics (e.g. Duley, 1939; Auzet et al., 1993), and could be used to infer soil hydrodynamic properties. Several classifications of the soil surface state have been developed (e.g. Boiffin et al., 1988) and used to understand runoff and erosion processes in various environments such as West and Sub-Saharan Africa (Casenave and Valentin, 1992; Valentin, 1991), Australia (Moss and Watson, 1991; Foley et al., 1991), Israel (Eldridge et al., 2000), USA (Baumhardt et al., 1991; Le Bissonnais and Singer, 1992), Iran (Eghbal et al., 1996) and Northern Europe (Auzet et al., 1995; Van Dijk and Kwaad, 1996; Le Bissonnais et al., 2005; Evrard et al., 2008). Numerous runoff and infiltration equations have been elaborated using these parameters (Seginer and Morin, 1969; Brakensiek and Rawls, 1983; Assouline and Mualem, 1996). Models using this approach demonstrated their ability to predict runoff and erosion in agricultural fields in various contexts on loess soils (e.g. in France and Belgium), suggesting that they adequately captured the main runoff dynamics drivers, as well as their temporal variations (Evrard et al., 2009). Most importantly, these studies provided a methodology to create soil hydrodynamic properties maps that may be used by physically based models (e.g. De Roo and Riezebos, 1992), and to account for their spatial and temporal variability. Soil surface state classes can also be directly be used to incorporate infiltration, imbibition (reflecting pre-ponding rainfall),

Manning's coefficient (Cerdan et al., 2002a), but also erosive parameters such as the potential suspended sediment concentration (Cerdan et al., 2002b) in expert based runoff and soil erosion models (Baartman et al., 2020).

However, even if monitoring soil surface state requires limited efforts and could be used to create adequate runoff model inputs, such monitoring strategies are time-consuming, which may not always be feasible (e.g. in remote catchments locations, for time and/or money constraints). The literature is therefore lacking means to account for the potentially high spatial and temporal variability of soil surface properties and to represent runoff dynamics in agricultural catchments.

Accordingly, the goal of our research was to develop and evaluate a parametrization software producing runoff and erosion model inputs: the PREMACHE (Parameterization of Runoff and Erosion Models in Agricultural Catchments) software. It provides users with an easy approach when using models to address the complex hydro-sedimentary behavior of agricultural catchments. This approach is based on the use of soil surface state as proxies of soil hydrodynamic properties the validity of which was demonstrated in the literature. A simple parameterization of soil surface state dynamics over common crop types is proposed, and evaluated in an agricultural catchment located in the European loess belt. Soil hydrodynamic properties, such as infiltration capacity, were deduced from the modeled soil surface state and literature data review. It was then used to analyze the impacts of the soil properties spatial and temporal heterogeneities on the catchment dynamics. Finally, the toolbox used to create runoff model inputs is provided with setup values along with the manuscript to support models parameterization for ungauged agricultural catchments.

2. Methods

2.1. Study area

The monitoring campaigns were performed in the Bourville catchment, located in Upper Normandy, France (Figure 1a), within the European loess belt, defined as the "Silt" and "Silt-loam" texture in the USDA classification applied to the dataset proposed by Ballabio et al. (2016). This site is a 1045 ha

catchment which was mainly covered, during the monitoring period of almost 9 years (September, 26th 2007 - May, 31th 2016) with cropland (72%), grassland (18%), urban (6%) and forested areas (4%). The main crops were, relative to the total crops area, wheat (42%), flax (16%), rapeseed (13%), sugar beet (7%), winter barley (7%), potatoes (6%) and maize (6%).

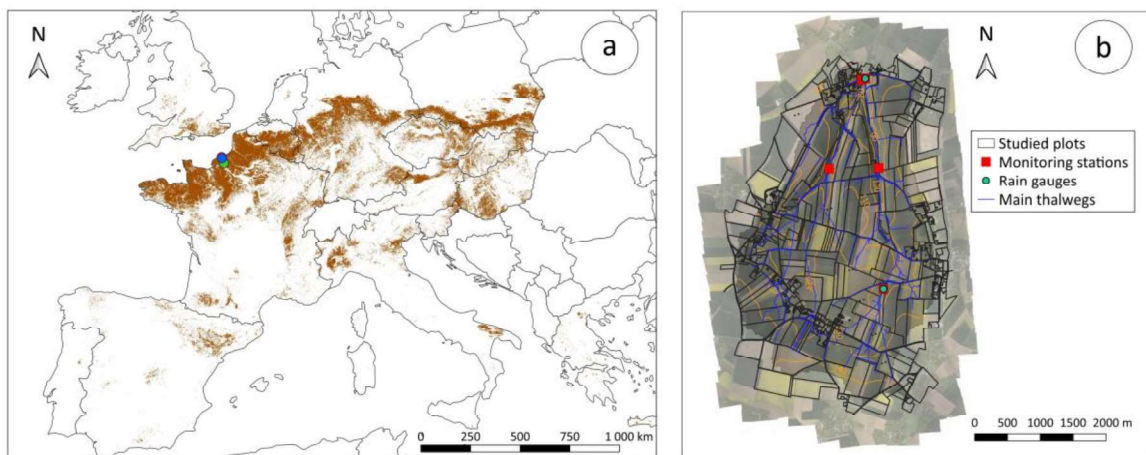


Figure 1: a) Location of the study area in Europe. The Bourville (blue) and nearby Blosseville (red) and Austreberthe (green) catchments are located within the European loess belt (brown areas). The experimental setup of the Bourville catchment is presented in subfigure b).

The catchment is mainly covered with Neoluvisol and Brunisol soils. According to the USDA soil textural classification, soils are referred to as silts and silt loams, associated with a low structural stability. These soils developed on well-drained thick soils, overlying karstic geological formation. Silt and silt loam corresponded to more than 9% of the surface area of the European soil texture dataset proposed by Ballabio et al. (2016), indicating that the studied catchment soils are representative of cultivated soils across the continent. These soil types have been described as sensitive to surface crusting, affecting the soil's hydrodynamic properties. Indeed, an increase in crusting results in a decrease of the infiltration capacity (Boiffin et al., 1988; Le Bissonnais et al., 1998). Additional data were also collected from literature for the nearby Blosseville and Austreberthe catchments (section 2.2.2): they were located 10 km north and 30 km south of the Bourville catchment, respectively. Both sites are covered with silt loam soils developed on loess Quaternary deposits. These catchments included a large

proportion of cultivated areas: more than 90% for the Blosseville catchment (90 ha) and 60% for the Autreberthe catchment (215 km²). Additional details on these catchments can be found in Cerdan et al. (2002a) and Delmas et al. (2012), respectively.

2.2. Field measurements

2.2.1. Crop type and soil surface state monitoring

On average during the monitoring period, 110 plots were surveyed in the Bourville catchment. The associated crops types, seeding, harvesting and tillage operations (e.g. ploughing) dates were determined through farmers' interviews and field observations. Crusting stage, crop cover and roughness were also monitored for 19 different crops following the procedure described in Boiffin et al. (1988) and Ludwig (1992). Two micro-plots (50 cm x 35 cm) were delimited in each plot, photographs were taken and observations were performed on the field to evaluate crop cover and surface roughness. The specific procedures described in Bresson and Boiffin (1990) were used to define the crusting stage. These procedures are based on morphological descriptions of clods size and shape, and estimation of inter-clods patches of continuous areas where interstices disappeared. These observations were performed at different periods to capture plant growth and crusting development. The corresponding crops and monitoring classes were reported in Table 1.

Crop cover index		Crusting		Roughness		Monitored crop types
C1	0 – 20 %	F0	Fragmentary	R0	0 - 1 cm	Wheat x 4 (N=42)
			stage			Flax x 2 (N=24)
C2	21 – 60 %	F1	Structural	R1	1 - 2 cm	Rapeseed x 2 (N=20)
			stage			Sugar beet x 2 (N=22)
C3	61 – 100 %	F12	Intermediate	R2	2 - 5 cm	Potatoes x 2 (N=18)
			crusting			Maize x 2 (N=16)
		F2	Sedimentary	R3	5 - 10 cm	Peas x 2 (N=14)
			crust			Intercrops x 3 (N=22)

Table 1: Soil surface state, associated nomenclature and crop types monitored for their soil surface state. The number of monitored plots and total observation numbers (in parenthesis, including the two locations and the temporal observations) are indicated in the last column.

The monitored crops represented the most common plants cultivated in the catchment (section 2.1). Several plots were monitored to include a variety of crop rotations type. For each monitored plot, the crop cover, crusting and roughness level were assessed for the two micro-plots and during various measurement periods to capture the entire growing cycle. Measurements were performed between four and seven times (on average five times) over the monitoring period, depending on the crop growing duration. In total, 176 observations were used for this study. Depending on the crop growing cycle duration, each crop type was monitored for a period comprised between 51 and 202 days (mean 126 days).

2.2.2. Additional soil surface state data

To increase the database robustness, the 204 observations on plots cultivated with wheat presented by Delmas et al. (2012) were used in the current research to generate the parameterization proposed in section 3.2 and 3.3. In the current research, results will be presented only for the main winter (i.e. wheat) and spring (i.e. flax) crop types observed in the Bourville catchment. Additional figures, showing parameterization performance for the other monitored crops, can be found in supplementary material for evaluation over a variety of crop types. Moreover, the parameterization was validated on measurements performed in the Blosseville catchment in section 3.4. The latter included rainfall and soil surface state observations on 20 plots at 5 to 6 dates along the entire crop cycle, corresponding to an additional 109 observations over an additional year. Results are also presented in supplementary material. In this study, 489 observations were used including 380 records for parameterization and 109 for validation. This compilation relied on observations made across three different catchments and contrasted monitoring periods, corresponded to three years of monitored data. It is therefore

expected that this compilation would produce results that can be extrapolated to other catchments, as it included various rainfall depths, intensity, kinetic energy, as well as variations in temperatures and soil textures.

2.3. Monitoring stations and data processing

Rainfall and water discharge were measured in the Bourville catchment. Measurement of water discharge was contemporary to rainfall period. Rainfall was monitored with automatic rain gauges at a 6-minutes time step (Précis Mécanique 3029) from September 2007 to May 2016. Mean annual rainfall was ranging from 629 mm to 974 mm, with a mean of 769 mm over the monitoring period. The mean long-term (1981-2010) annual rainfall recorded at the nearby Le Havre station is 790 mm with a mean monthly rainfall ranged from 52 mm (February) to 89 mm (December). The monitored rainfall is therefore representing average conditions, including both dry and wet years.

Water discharge was measured at four locations in the catchments, including nested measurements in sub-catchments. In this study, we only used data from the station located at the catchment outlet. Discharge was measured using a calibrated flume, using water height probes (INW PT12) measuring water height at a high frequency, and recorded using a ISCO 2105G data logger. The monitoring frequency ranged from one to six minutes, depending on the monitoring period. Gauging was performed using a velocimeter (Valport 801 flat) or the salt dilution method, depending on the discharge range. Gauging was combined with water height levels to establish rating curves (Richet et al., 2021), resulting in high-frequency discharge monitoring at each station. The rating curve fitted well with the 13 measurements; the determination coefficient was 0.99 at the catchment outlet. Measured discharge ranged from $0.04 \text{ m}^3 \cdot \text{s}^{-1}$ to $2.7 \text{ m}^3 \cdot \text{s}^{-1}$. 95.7% of the values recorded during the monitoring period were included in this range, indicating its representativity. Field observations lead since 1994 did not revealed any spring in the catchment, and it had no watercourses, only ditches (Richet et al., 2021). Therefore, the measured discharge results only from runoff.

Individual rainfall events were defined from the rainfall time series measured at a 6-minutes time step. One individual event was defined as more than 1 mm of rain, separated from the following event by at least 3 hours without rainfall. Rainfall depth, duration and intensity were then calculated for each rainfall event. Individual runoff events were defined from the discharge time series as events with a peak discharge higher than $0.03 \text{ m}^3 \cdot \text{s}^{-1}$ and a total volume higher than 0.01 mm. Runoff volume, duration, peak discharge were calculated for analyzing the catchment hydrological dynamics (performed in Richet et al., 2021). This procedure was adapted from the methodology proposed by Grangeon et al. (2021). The parametrization developed in this study made use of rainfall depth and intensity during the rainfall events, as well as rainfall depth occurring prior to runoff events, considered a proxy of soil moisture (Cerdan et al., 2002).

The Mood test was used at the 5% level of significance to test for median differences between groups in rainfall and runoff distributions. To assess the parameterization performance, the Kruskal-Wallis test was used at the 5% level of significance.

2.4. PREMACHE framework description

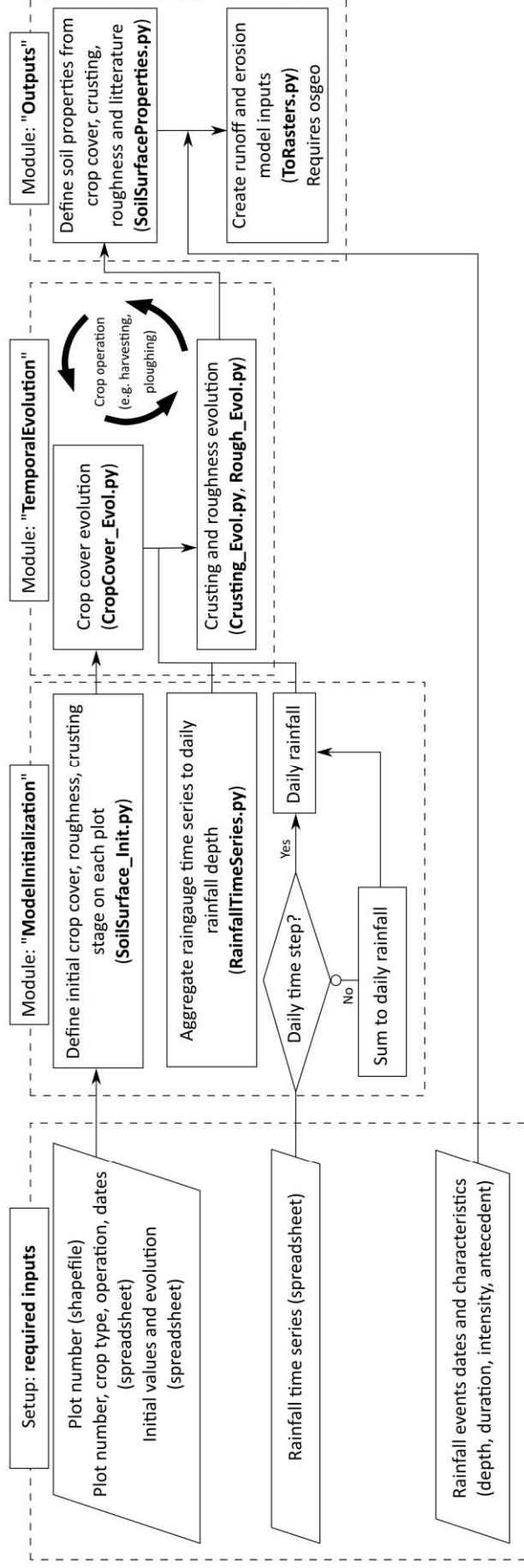
2.4.1. Model summary

The objective of the PREMACHE software was to generate soil hydrodynamic property maps that can be readily used as runoff and erosion models inputs. The following model inputs can be created at a daily time step: infiltration capacity, imbibition and Manning's n coefficient. Additional variables related to erosion modelling are also provided (sheet erosion concentration and soil erodibility), based on the data proposed by Cerdan et al. (2002b). However, in this study, results will focus on infiltration capacity, as it is one of the main runoff model requirements.

To create a spatial distribution of these parameters (maps), the soil surface state is modeled by PREMACHE at a daily time step, on each plot across the catchment. For each plot, PREMACHE initialized the crop cover, crusting and roughness based on empirical data depending on the crop type, previous shallow tillage operations and potential chemical crop destruction. Crop cover was then modeled to

234 increase with time over the modeled period, depending on the crop type. Empirical data from the
235 current study was provided as default values for different crop type. PREMACHE then combined the
236 crop cover with rainfall records to model soil crusting and roughness evolution. Crop operations are
237 considered, as they may modify both crop cover (e.g. harvesting) and surface crusting and roughness
238 through tillage operations (e.g. ploughing).

239 Finally, conversion of soil surface states into hydrodynamic properties was performed using the
240 procedure described in the STREAM model (Cerdan et al., 2002a). The Manning coefficient was derived
241 from the experimental data proposed for various crop types by Gilley et al. (1991) and Morgan (2005).
242 These values can also be modified on the corresponding input spreadsheet. The software functioning
243 is summarized in Figure 2.



Values acquired in the current study are provided with the toolbox and may be used as default values in similar although unmonitored catchments. Otherwise, values can be modified in the spreadsheets to reflect changes in soil properties for instance.

The GIS files were processed using QGIS (QGIS, 2022; V.3.10 - A Coruña). The toolbox was developed as a sequence of scripts using Python V.3.8.5 and is available at <https://github.com/BRGM/premache>

2.4.2. Required inputs

The required inputs are:

- A raster providing the expected resolution and extent, such as the Digital Elevation Model (DEM).
- A shapefile corresponding to the catchment plots. Each plot should be associated with a plot (arbitrary) number. As the plot sizes and locations may change over time, multiple shapefiles can be used to reflect the land use temporal evolution. Monitored data, national databases providing annual maps or statistics can be used to fill in this spreadsheet.
- A spreadsheet file indicating the land use (including crop type and farming operations) at each measurement period, with the associated plot numbers.
- A two-column file including the rain gauge records. Rainfall records should be provided with a daily time step. If a higher resolution is available, the toolbox can be used to decrease the resolution to a daily time step in order to avoid high frequency variations while conserving an adequate temporal resolution regarding the timescales involved in the control of soil surface state evolution.
- A file including rainfall events characteristics for which runoff model inputs will be generated. Users should provide one or multiple dates of interest in a specific file, corresponding to rainfall events that should be modeled, with their associated characteristics: rainfall depth, duration maximum intensity and rainfall depth over the past two days before the rainfall event.

- Three different tables describing the evolution of:
 - Crop cover increase as a function of time and crop cover decrease dynamics under different farming operation types. In the current research, ploughing and chemical destruction were considered separately, as described below (section 3.2).
 - Surface roughness and crusting as a function of both cumulative rainfall and crop cover (section 3.3).

2.4.3. Limitations and adaptations

In the toolbox, crops are assumed to grow independently from rainfall and temperature. Our dataset, and the corresponding parameterization, should therefore need additional calibration for catchments undergoing severe dry or wet periods. We are also aware that process-based approaches were proposed in the literature (Peñuela et al., 2018; Boas et al., 2021), for instance to model crop growing at various scales. However, the goal of the current research was to provide measurement data and a simple parameterization to obtain reliable estimates of soil surface evolution, based on limited input requirements. Moreover, the software made use of simple spreadsheets; values can therefore be easily modified according to the scientists' knowledge, or using dedicated measurements or more detailed crop growing modelling.

This toolbox was developed for agricultural fields on soils prone to surface crusting, and may therefore need additional calibration to describe soil surface evolution in catchment located in a different climate context and on different soils (i.e. loess-derived silt-sized soils) than those typically found in the European loess belt, for instance following the methodology proposed in Ludwig (1992) or Evrard et al. (2009). While it should help modelers in representing soils hydrodynamics properties, they should adapt the proposed values depending on the dominant processes occurring in the modeled catchment. It should also be noted that this approach was successfully adapted by Gascuel-Oudou et al. (2009) and Evrard et al. (2009) for catchments of Western France, Southern France and Belgium, suggesting that it may be implemented in catchments located in other regions.

3. Results and discussion

3.1. Rainfall and crop types variations over the monitoring period

During the monitoring period, 227 runoff events were recorded. Among them, 40 (18%) events occurred after a rainfall depth lower than 5 mm, 187 events (82%) took place in response to rainfall depths higher than 5 mm, including 104 (47%) runoff events occurring following rainfall depths higher than 10 mm (Figure 3).

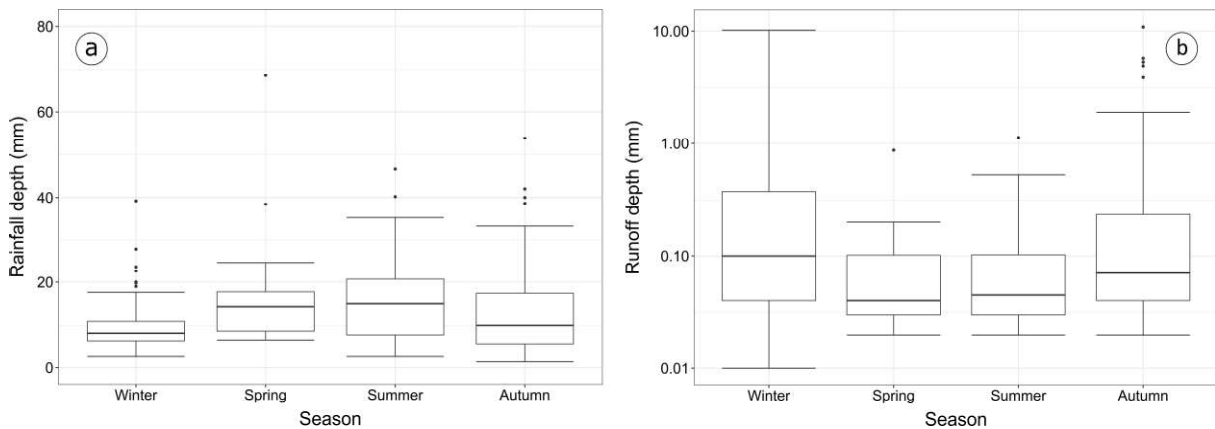


Figure 3: Boxplots of a) rainfall depth that resulted in runoff events and b) corresponding runoff depth (logarithmic scale in the y-axis).

Most runoff events (Figure 3b) occurred during autumn (49%) and winter (31%). Runoff events were also recorded during summer (14%) and spring (6%). Interestingly, a significantly higher rainfall depth was required to generate runoff event in summer than in winter: the corresponding median rainfall depths amounted to 15 mm and 8.2 mm, respectively (Figure 3a), and the median runoff depth amounted 0.05 mm and 0.1 mm, respectively (Figure 3b). In this case, runoff occurrence is related to the high variability in infiltration capacity over seasons resulting from surface crusting, with infiltration rates ranging from 2 mm.h⁻¹ to 50 mm.h⁻¹ (Cerdan et al., 2002a).

The evolution of crop types over the monitoring period is provided in Figure 4.

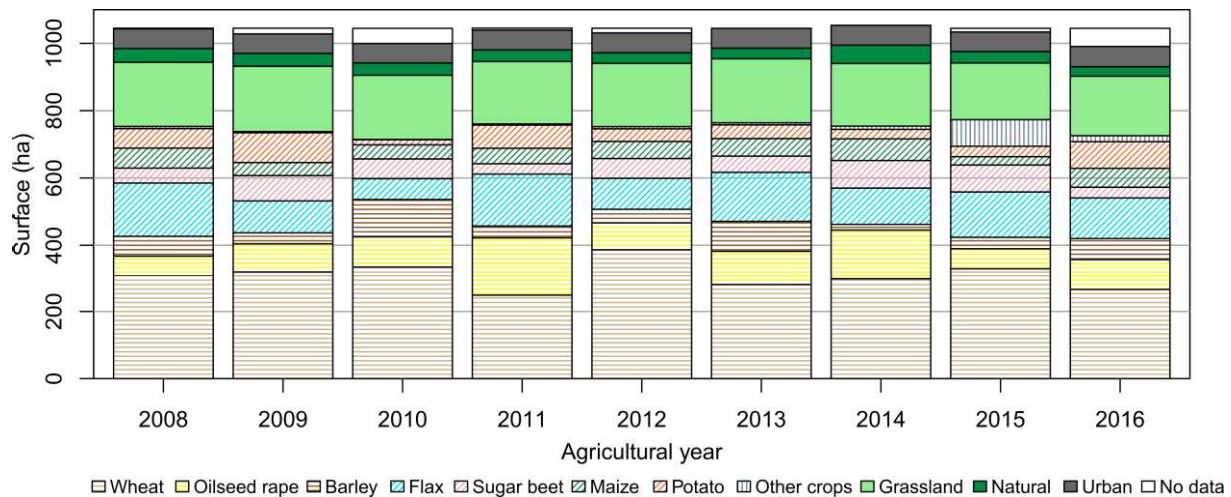


Figure 4: Crop type evolution during the monitoring period. Each year is corresponding to agricultural years, starting in September, e.g. “2008” is corresponding to 1st September 2007 to 31 August 2008. Intercrops were not included in this analysis. No data values corresponded to periods when it was not possible to collect data from landowners.

The cultivated areas were dominated by winter crops (60%), including wheat, rapeseed and winter barley. Spring crops, including flax, sugar beet, maize and potatoes, represented 35% of the cultivated area. These crops were also the most widely cultivated plants crops in Europe for the period 2009-2019, and including common wheat, maize and corn-cob mix, barley, oats and rye (Eurostat, 2019). The observed crops are therefore representative of the most commonly cultivated plants in Europe.

The current study took advantage of extensive field measurements obtained with the active cooperation of landowners. Consequently, a unique long-term monitoring of crop types and shallow tillage operations was available for this study. At large scales, such data are usually not available, but interesting approaches such as crop rotation simulations (Schönhart et al., 2011; Sietz et al., 2021) may contribute to improve such shortcomings. The proposed database from our study may be used to validate such approaches.

3.2. Crop cover evolution

Crop cover evolution was evaluated over the entire catchment based the soil surface state observation. The mean seeding date corresponded to mean values obtained from the farmers' interviews. The resulting crop cover evolution is proposed in Table 2.

Crop cover	Mean seeding date	20%	40%	60%	80%	100%
Crop cover class	(0 %)					
	C1		C2		C3	
Crop type	Crops growing (days)					
Sugar beets, cabbages, spinach	April 15 th	44	75	83	102	107
Maize	April 25 th	66	82	92	114	124
Flax, alfalfa	March 15 th	29	48	58	76	81
Peas, faba beans, beans	March 30 th	55	76	87	93	103
Potatoes	April 15 th	45	65	72	88	93
Oats, rye, radish	April 10 th	25	45	55	61	66
Wheat	October 20 th	92	136	186	193	203
Barley	October 5 th	77	154	176	198	208
Rapeseed	September 5 th	61	77	207	210	215
Ryegrass, clover	September 5 th	40	57	71	73	107
Intercrops with mustard	September 5 th	30	45	55	57	64
Intercrops with phacelia	September 1 st	39	54	64	72	82
Intercrops: mustard or faba bean		d+50	d+30	d+20	d+10	d
Intercrops: other types		d+50	d+35	d+25	d+15	d

Table 2 : Soil cover parameterization deduced from the field survey. Numbers indicate the days required to reach the corresponding crop cover. The “d” letter corresponded to crops destruction.

Crop cover was divided into 5 segments (0% to 100% in 20% increments) to allow for a smoother transition between classes, particularly for crusting and roughness evolutions (see section 3.3 below). However, they were aggregated in three classes (0%-20%; 21%-60%; 61%-100%) for comparison with measurements. After the progressive crop cover increase during the growing period, different operations were considered for explaining the crop cover decrease: chemical destruction, harvesting, mechanical destruction, and ploughing. Intercrop chemical destruction was estimated to result in a progressive decrease from a fully developed crop or intercrop to a limited cover in 50 days (Martin, 1997). Conversely, harvesting and ploughing resulted in a quick decrease from a maximal to a limited crop cover. The initial crop cover of the following crop type was therefore defined based on the previous crop type and latest farming operation. An illustration of the modeled and observed crop covers for the two most common winter and spring crops is provided in Figure 5. For evaluation over other crop types and on the Blosseville catchment, additional figures were provided as supplementary material.

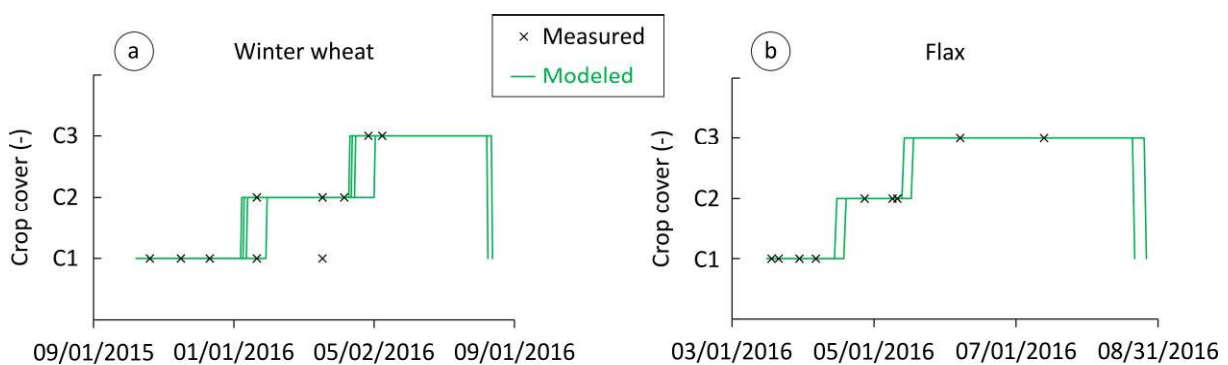


Figure 5: Measured (black crosses) and modeled (green continuous line) crop cover for the two most common crops observed in the catchment: a) winter wheat (four plots were monitored) and b) flax (two plots were monitored). The different lines corresponded to different modeled plots. The differences between lines is linked to differences in seeding dates.

The modeled crop cover over the eight crop types detailed in Table 1 matched the observation for 73% of the records, indicating a good parameterization performance. The agreement between modeled and measured values was statistically significant. It should however be noticed that some temporal variability was observed. For instance, the measured crop cover for winter wheat varied between C1 (0% - 20%) and C2 (21% - 60%) from 21st January to 18th March (Figure 5a), depending on the monitored plots. It indicated some inherent variability in crop cover that was only partly explained by the differences in seeding dates, reflected by the modeled variability between plots (e.g. maize; supplementary material). Interestingly, the proposed values were in agreement with data collected in the literature in various contexts. For instance, Tang et al. (2018) measured that the crop cover was maximal for winter wheat approximately 180 days after sowing, while our measurements indicated a corresponding period of approximately 190 days. Deng et al. (2012) indicated that the maximal plant growth was measured after 90 days for flax and 140 days for maize, while we found in our study values of 80 and 130 days, respectively. The agreement in ranges between the values proposed in this study and the results reported in the literature suggest that the simple approach proposed in this study may be applied to other catchments to obtain reliable although rough estimates of crop growing.

3.3. Soil crusting and roughness evolution

The initial values for roughness and surface crusting depend on the previous (inter-)crop type and crop operation. For instance, ploughing results in a high surface roughness (i.e. > 10 cm), a value that may also be observed for potato crops. Therefore, for each crop type, the initial surface roughness and surface crusting were assumed to be controlled by the previous crop operation (e.g. ploughing, mechanical destruction) and the current crop type. In addition to this temporal evolution, initial values for crusting and roughness were therefore proposed and included as inputs for each crop type.

In this study, a parameterization of crusting and roughness evolution based on daily rainfall data (Ndiaye et al., 2005; Vinci et al., 2020) was proposed, taking into account the protective effects of the crop cover. Indeed, increasing the soil cover by vegetation was demonstrated to reduce the rainfall

kinetic energy (e.g. Brandt et al., 1989) and, therefore, the soil aggregate breakdown, limiting crusting and roughness decrease. The parameterization, including Table 2 and Table 3, was initially based on expert knowledge acquired in this region during the past decades (e.g. Auzet et al., 1990; Ouvry and Ligneau, 1993, Martin et al., 2010), and was then adapted using the measurements acquired during this study and collected from Delmas et al. (2012). The resulting parameterization is proposed in Table 3 to define roughness and crusting evolution over time and rainfall for various crop covers (as defined in section 3.2).

Crop cover		0%-20%	20%-40%	40%-60%	60%-80%	80%-100%
Surface roughness	R4 → R3	150	190	225	300	375
	R3 → R2	120	150	180	240	300
	R2 → R1	120	150	180	240	300
	R1 → R0	120	150	180	240	300
Surface crusting	F0 → F1	30	45	90	115	120
	F1 → F12	35	50	100	125	130
	F12 → F2	90	130	265	335	350

Table 3: Soil roughness and crusting evolution under rainfall. The numbers indicate the rainfall depth (mm) required to reach the corresponding roughness or crusting stage, for each crop cover class (columns).

An illustration of the proposed parameterization and comparison with measurements for crusting stages and soil roughness is presented in Figure 6. Additional figures presented as supplementary material presented the parameterization results for other crop types.

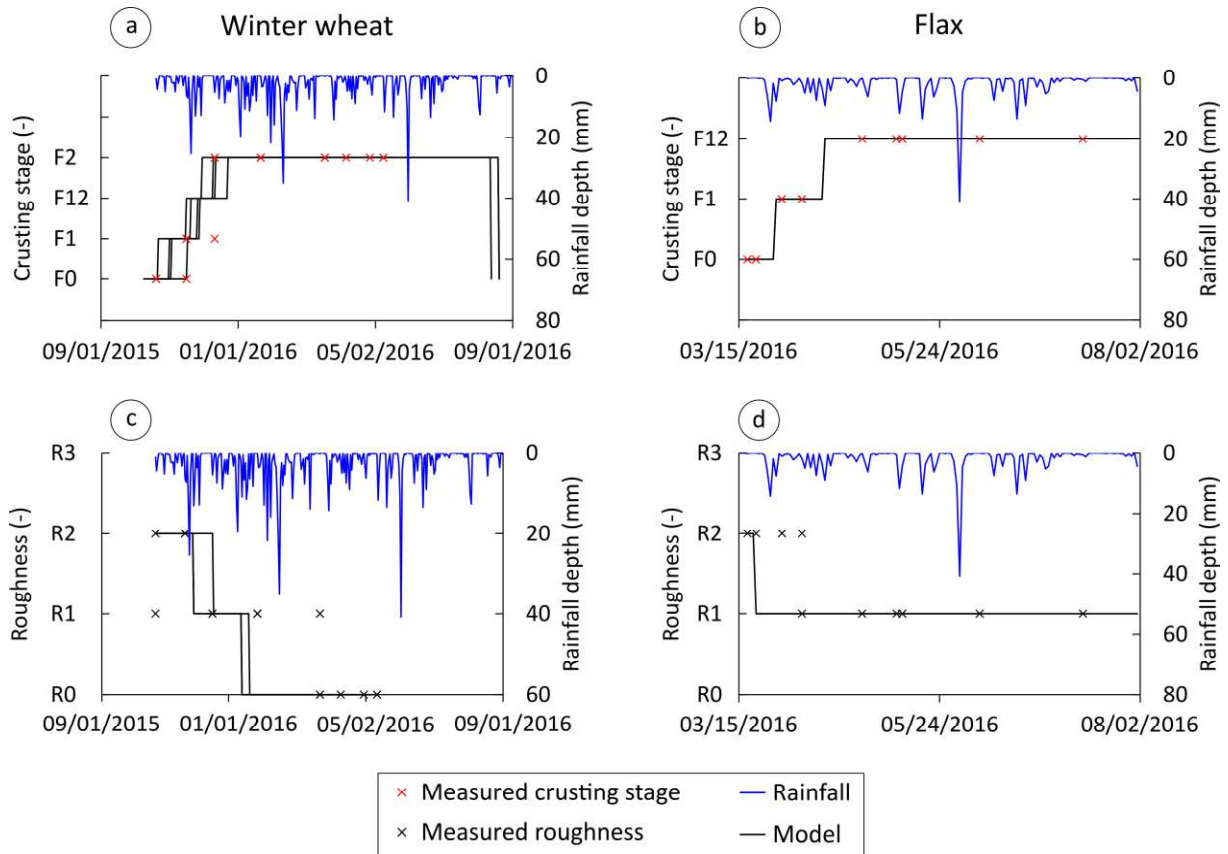


Figure 6: Measured (crosses) and modeled (continuous line) crusting stage (a and b, red crosses) and soil roughness (c and d, black crosses) for winter wheat and flax. The continuous blue line represents daily rainfall.

The agreement between observed and modeled values reached 63% for the crusting stage and 74% for the roughness, and was statistically significant. The limited performance for crusting is partly explained by the poor performance obtained for fields cultivated with potatoes (22%, p-value=0.24). This is related to the limited crop cover in the early stages of plant growth, the modeled crusting stage quickly increased to reach the stage of crusted soil with sedimentary crust (F2). However, crusting is assumed to remain limited on inter-rows, as reflected by measurements indicating the occurrence of a structural stage (F1) during 72% of the monitoring period, ranging from April to August for this crop type, and that of intermediate crusting (F12) as maximal observed crusting stage. Therefore, the parameterization performance remained low for this crop type. Consequently, crusting evolution for soil surface with high initial roughness (R4) should be considered with caution, and further developments should include a relationship between crusting and roughness.

3.4. Evaluation of the parameterization extrapolation abilities

In addition to parameterization evaluation as performed in sections 3.2 and 3.3, we assessed whether the PREMACHE framework could be applied to other catchments by using the 109 observations of the Blosseville catchment. Results from the Blosseville catchments are presented in supplementary material. For the 20 monitored plots covered with wheat (7 plots), flax (2 plots), peas (3 plots) and winter barley (3 plots), the predicted crop cover was good. The modeled values corresponded to measurements in 91% of the cases. Errors were observed regarding the occurrence of intermediate crop cover (C2) on fields planted with peas and wheat. For crusting, only data for fields cultivated with flax and peas were available, and the parameterization matched the observations in 87% of the cases, with the few errors occurring regarding the prediction of the structural crusting stage (F1). Finally, for roughness, the parameterization performance was acceptable, with 82% of agreement between observations and modeled values, mainly due to errors to predict the roughness early stages for fields planted with wheat and winter barley: after seeding (occurring the 8th October) the observations indicated a limited roughness (R1) while the parameterization predicted a slightly higher roughness (R2) until mid-December. However, given the variations observed in the measurements, the model performance could be considered as acceptable.

3.5. Implications for runoff modelling

Adequately representing the variability of soil hydrodynamic properties, such as infiltration capacity, is a long-standing issue for runoff modelers. Moreover, in agricultural catchments, the significance of shallow tillage operations can dramatically change these properties within a very short period of time (Martin et al., 2004). The PREMACHE software proposes an alternative method to account for these variations in runoff modelling, which may be crucial in understanding catchments hydrological behavior (Wagner et al., 2019). As an illustrative example of the approach, the Bourville catchment mean infiltration capacity was modeled over two entire crop cycles. Calculations were performed from 1st September 2014 to 1st September 2016. For readability purpose, results are presented for 1st September 2014 to 1st June 2016, corresponding to a total of 253 rainfall events, as no significant runoff

event was recorded after 1st June 2016. For each of these rainfall events, the mean infiltration capacity, weighted by the plot surface, was reported. The link between infiltration capacity and runoff was visually suggested by indicating periods when runoff events were measured at the catchment outlet (Figure 7).

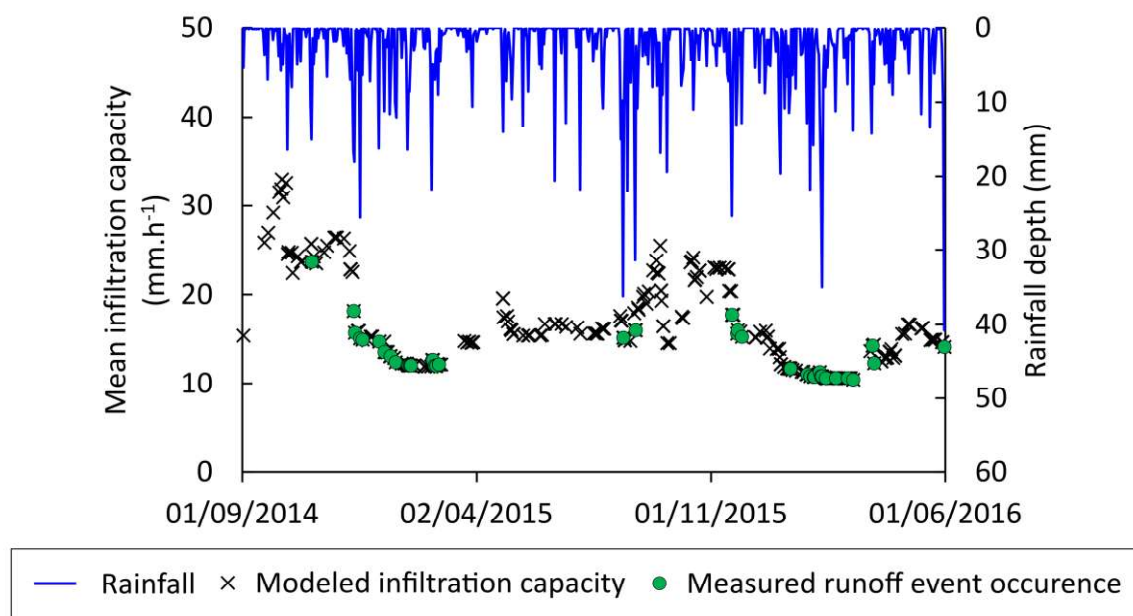


Figure 7: Modeled mean weighted infiltration capacity (black crosses) for each measured rainfall event and daily rainfall (blue continuous line) in the Bourville catchment. Green circles indicate when rainfall events generated a runoff event that was measured at the catchment outlet.

This result illustrated the dynamics of soil infiltration capacity and its impact on the catchment runoff dynamics. From November 2014 to February 2015, 41 rainfall events with a rainfall depth higher than 1 mm were recorded over 92 days. Consequently, soil crusting progressively increased, resulting in a decreased infiltration capacity, from 33 mm.h⁻¹ to 12 mm.h⁻¹, with direct implications for runoff generation (Ndiaye et al., 2005). This decrease occurred mainly because of three major storm events accumulating 60.2 mm. On some cultivated fields, infiltration capacity dropped from 50 mm.h⁻¹ in November 2014 to 2 mm.h⁻¹ in February 2015. This indicated that the soils were crusted with the occurrence of a sedimentary crust, resulting in a very limited infiltration capacity. After harvesting and spring crops seeding, crop cover decreased and crusting removal through shallow tillage operations

resulted in an increased infiltration capacity, up to 26 mm.h⁻¹ (November 2015). This increase underlined the importance of shallow tillage operations in controlling the infiltration rates of the catchment and, more generally, on soil properties (Strudley et al., 2008). Future developments may include the effects of the tillage type (Osunbitan et al., 2005) and long-term farming methods (Basche and DeLonge, 2019).

Then, an unusually wet period occurred in September 2015 resulted in widespread soil crusting. The mean infiltration capacity decreased again to 15 mm.h⁻¹. Rainfall depth was 87.8 mm in September 2015 while the measured mean was 56 mm. Shallow tillage operations performed across multiple fields had a strong influence on the catchment-scale infiltration capacity (Martin et al., 2010). It increased soil infiltration capacity to 24 mm.h⁻¹ in October 2015, followed by another progressive decrease during winter. This high-frequency result indicated that the soils' hydrodynamics might exhibit quick variations due to the combination of rainfall and tillage operations and may be taken into account with the simple parameterization proposed in the current research.

Interestingly, this result illustrates the dominance of infiltration-excess runoff. Runoff events, as defined in section 2.3 (i.e. based on a threshold on runoff volume and discharge peak), occurred mainly when rainfall increased crusting, resulting in a mean infiltration capacity below 20 mm.h⁻¹. The PREMACHE software may therefore be used to provide inputs for runoff and erosion models and to increase their performance by taking into account the fast (e.g. progressive crusting in winter and tillage operations) and long-term (cycles over multiple years) dynamics of soil infiltration capacity. It therefore offers a possibility to quantify the infiltration-runoff partition and could therefore complement existing modelling approaches such as that including curve number variations in models (Mehdi et al., 2015). This may be useful in agricultural catchments, as both infiltration-excess and saturation-excess may be involved in generating flood events in such environments (Saffarpour et al., 2016; Grangeon et al., 2021).

In addition to the temporal dynamics, it is also important to consider the spatial variations of infiltration capacity at the catchment scale (Figure 8).

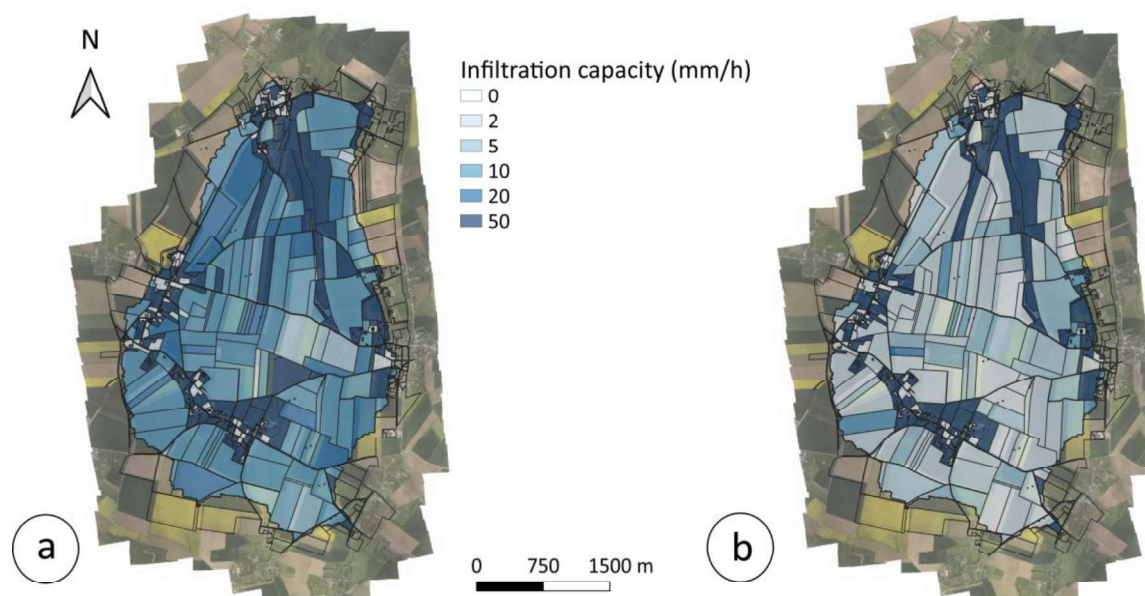


Figure 8: Spatial distribution of infiltration capacity in the Bourville catchment, as simulated by the PREMACHE software in a) November 2015 (mean infiltration capacity: 33 mm.h⁻¹) and b) February 2016 (mean infiltration capacity: 12 mm.h⁻¹).

Plot-to-plot variations was mainly related to differences in crop types and soil surface states. These spatial variations have important implications for runoff triggering. In particular, grasslands, characterized by a high infiltration capacity (in this study, 50 mm.h⁻¹), were located in a talweg in the northern part of the Bourville catchment, concentrating runoff at locations with a high infiltration capacity. It will therefore decrease runoff volumes recorded at the outlet regardless the considered season. Depending on the considered rainfall events, it might affect the areas producing runoff and those infiltrating the runoff volumes, therefore affecting the hydrological connectivity (Darboux et al., 2001), which was previously demonstrated to be affected by landscape patchiness (e.g. Baartman et al., 2020). Of note, specific cases such as the effects of grazing on pastures infiltration capacity (Joannon, 2004) were not included in this analysis. However, they can be accounted for by creating a dedicated field in the toolbox.

The current study proposed an approach to account for spatiotemporal variations in soil hydrodynamic properties in complex catchments including agricultural areas. Based on simple inputs, it is complementary to existing modelling approaches in that it can also incorporate other knowledge or model inputs.

4. Conclusions

In the current research, existing knowledge on soil surface state and a unique database were compiled. The database included the monitoring of crop types and soil surface state, as well as the high-resolution measurement of rainfall and runoff. Although the monitored sites corresponded to loamy soils sensitive to surface crusting under temperate climatic conditions, they may be representative of the conditions observed in other cultivated regions where hydrological processes are dominated by infiltration-excess runoff.

A framework describing the soil surface state dynamics was developed and included in a software made available for download. It made use of limited field data inputs: crop types and tillage operations at different observation dates, and rainfall time series. It was demonstrated to adequately reproduce the changes in crop cover, soil crusting and roughness on various crop types, in two different catchments. Previous research results were used to convert these soil surface states into hydrodynamic properties such as infiltration capacity. The software used in this study was made available for download and can be used to support runoff modelling in agricultural catchments where experimental data are lacking, using either the proposed default values or modifications based on modeler's knowledge.

When applied to the studied catchment, results demonstrated the high variability of soil infiltration capacity between crop types, depending on the sequences of tillage operations and rainfall dynamics. The variations in infiltration capacity at the catchment scale and for various time scales, from the rainfall event to the inter-annual scale, and its strong implications for runoff modelling were illustrated. The proposed approach allows representing this variability in runoff models by creating runoff model

513 inputs, based on a large database proposed along with the manuscript. It may therefore be useful for
514 applications in unmonitored agricultural areas in general and more specifically on loamy soils,
515 susceptible to crusting. It will help representing the temporal and spatial variability of soils
516 hydrodynamic properties for different crops and a sequence of hydrological years, which will
517 ultimately contribute to a better understanding of runoff pathways and hydrological connectivity at
518 the catchment scale.

Acknowledgments: The general idea of this manuscript, based on soil surface state, largely originated from the pioneering work of late Yves Le Bissonnais. We would particularly like to thank the landowners for their involvement in the data collection and for granting access to their fields, making this long-term work possible: Mrs. Baret, Bazire, Bouclon, Burel, Cabot, Constantin, Cordier, Delafontaine, Delamare, Delaunay, Grindel, Laguerre, Larcher, Lefrançois, Martine, Mignot, Moonen van Meer, Olivier, Pesqueux, Petit, Planchon, Poulet, Rossignol, Roussel, Terrier and Voisin. The assistance of Mathieu Saulnier in field measurements is acknowledged. Thomas Grangeon would like to thank Farid Smai and Theophile Guillon for their help in model formatting and GitHub deposit. The two anonymous reviewers provided constructive and detailed comments that helped improving the manuscript quality.

Funding: The monitoring of the Bourville catchment was supported by the Seine Normandy Water Agency within the framework of the Pesticeros project.

This work has been supported by the French State financial support managed by the Agence Nationale de la Recherche, allocated in the “Investissements d’Avenir” framework programme under reference ANR-11-RSNR-0002 (AMORAD project).

Author contributions: JFO initiated the data acquisition on the Bourville catchment and secured the essential, yet uncommon, long-term funding needed to acquire representative measurements. JFO, LTP and JBR performed the crop observations, soil surface state measurements and farmers’ interviews. PM and OC provided additional experimental data for model calibration and validation. JFO, OC and JBR created the model parameterization, further modified by TG, RV and OC. TG, RV and LTP processed the rainfall and runoff data. RV wrote the first model version, further modified by TG. TG wrote the manuscript. All co-authors commented the manuscript.

Software and data availability: The data used in this study (Excel spreadsheets and shapefiles) and the PREMACHE toolbox are available at <https://github.com/BRGM/premache>.

543 PREMACHE is licensed under GPL V3.0. It was developed by Rosalie Vandromme and Thomas Grangeon
544 (r.vandromme@brgm.fr and t.grangeon@brgm.fr) in early 2021 under Python 3.8.5, using Windows
545 10, a 2.5 GHz i5-7300HQ CPU with 16 Go memory. Using this configuration, the model processed the
546 dataset proposed with the manuscript (a shapefile including approximately 1200 polygons monitored
547 over 9 years) and exported rasters at a 5 m resolution for a subset of 50 rainfall events in approximately
548 15 minutes.

549 References

- 550 Arnold J. G., Srinivasan R., Muttiah R.S., Williams J. R. (1998). Large area hydrologic modeling and
 551 assessment—Part 1: Model development. *Journal of the American Water Resources Association*,
 552 **34(1)**:73-89.
- 553 Assouline S., Mualem Y. (1997). Modeling the dynamics of seal formation and its effect on infiltration
 554 as related to soil and rainfall characteristics. *Water Resources Research*, **33(7)**:1527-1536.
- 555 Auzet A.V., Boiffin J., Papy F., Maucorps J., Ouvry J.F. (1990). An approach to the assessment of erosion
 556 forms and erosion risk on agricultural land in the northern Paris Basin, France. In: Boardman J., Foster
 557 I.D.L., Dearing J.A. (Eds.), *Soil Erosion on Agricultural Land*. Wiley, Chichester, UK, pp. 383–400
- 558 Auzet A.V., Boiffin J., Papy F., Ludwig B., Maucorps J. (1993). Rill erosion as a function of the
 559 characteristics of cultivated catchments in the North of France. *Catena*, **20**:41-62.
- 560 Auzet A.V., Boiffin J., Ludwig B. (1995). Concentrated flow erosion in cultivated catchments: influence
 561 of soil surface state. *Earth Surface Processes and Landforms*, **20(8)**:759-767.
- 562 Baartman J.E.L., Nunes J.P., Masselink R., Darboux F., Biëlders C., Degré A., Cantreul V., Cerdan O.,
 563 Grangeon T., Fiener P., Wilken F., Schindewolf M., Wainwright J. (2020). What do models tell us about
 564 water and sediment connectivity? *Geomorphology*, **367**:107300.
- 565 Basche A.D., DeLonge M.S. (2019). Comparing infiltration rates in soils managed with conventional and
 566 alternative farming methods: A meta-analysis. *PLoS ONE*, **14(9)**:e0215702.
- 567 Baumhardt R.L., Romkens M.J.M., Parlange J.Y., Whisler F.D. (1991). Predicting soil-surface seal
 568 conductance from incipient ponding and infiltration data. *Journal of Hydrology*, **128(1-4)**:277-291.
- 569 Ballabio C., Panagos P., Montanarella L. (2016). Mapping topsoil physical properties at European scale
 570 using the LUCAS database. *Geoderma*, **261**:110-123.

571 Bieger K., Arnold J.G., Rathjens H., White M.J., Bosch D.D., Allen P.M., Volk M., Srinivasan R. (2017).
 572 Introduction to SWAT+, a completely restructures version of the Soil and Water Assessment Tool.
 573 *Journal of the American Water Resources Association*, **53(1)**:115-130.

574 Boardman, J., Ligneau, L., de Roo, A., Vandaele, K., (1994). Flooding of property by runoff from
 575 agricultural land in northwestern Europe. *Geomorphology*, **10**:183–196.

576 Boardman, J. (2010). A short history of muddy floods. *Land Degradation & Development*, **21**:303-309.

577 Boardman J. (2020). A 38-year record of muddy flooding at Breaky Bottom: Learning from a detailed
 578 case study. *Catena*, **189**:104493.

579 Boas T., Bogena H., Grünwald T., Heinesch B., Ryu D., Schmidt M., Vereecken H., Western A., Franssen
 580 H.J.H. (2021). Improving the representation of cropland sites in the Community Land Model (CLM)
 581 version 5.0. *Geoscientific Model Development*, **14**:573-601.

582 Boiffin J., Papy F., Eimberck M. (1988). Influence des systèmes de culture sur les risques d'érosion par
 583 ruissellement concentré : I. Analyse des conditions de déclenchement de l'érosion. *Agronomie* **8**:663–
 584 673.

585 Brakensiek D.L., Rawls W.A. (1983). Agricultural management effects on soil water processes. Part II.
 586 Green and Ampt parameters for crusting soils. *Transactions of the ASAE*, **26(6)**:1753 1757

587 Brandt C.J. (1989). The size distribution of throughfall drops under vegetation canopies. *Catena*
 588 **16**:507–524.

589 Bresson L.M., Boiffin J. (1990). Morphological characterisation of soil crust development stages on an
 590 experimental field. *Geoderma*, **47**:301–325.

591 Casenave A., Valentin C. (1992). A runoff capability classification-system based on surface-features
 592 criteria in semiarid areas of West Africa. *Journal of Hydrology*, **130(1-4)**:231-249.

593 Cerdan O., Souchère V., Leconte V., Couturier A., Le Bissonnais Y. (2002a). Incorporating soil surface
594 crusting processes in an expert-based runoff model: Sealing and Transfer by Runoff and Erosion related
595 to Agricultural Management. *Catena*, **46**:189-205.

596 Cerdan O., Le Bissonnais Y., Couturier A., Saby N. (2002b). Modelling interrill erosion in small cultivated
597 catchments. *Hydrological Processes*, **16**:3215-3226.

598 Cerdan O., Le Bissonnais Y., Govers G., Lecomte V., van Oost K., Couturier A., King C., Dubreuil N. (2004).
599 Scale effect on runoff from experimental plots to catchments in agricultural areas in Normandy. *Journal*
600 *of Hydrology*, **299(1-2)**:4-14.

601 Darboux F., Davy P., Gascuel-Oudou C., Huang C. (2001). Evolution of soil surface roughness and
602 flowpath connectivity in overland flow experiments. *Catena*, **46**:125-139.

603 Delmas M., Pak L.T., Cerdan O., Souchère V., Le Bissonnais Y., Couturier A., Sorel L. (2012). Erosion and
604 sediment budget across scale: A case study in a catchment of European loess belt. *Journal of Hydrology*,
605 **420-421**:255-263.

606 De Roo A.P.J., Riezebos H.T. (1992). Infiltration experiments on loess soils and their implications for
607 modeling surface runoff and soil erosion. *Catena*, **19(2)**:221-239.

608 De Roo A.P.J., Wesseling C.G., Ritsema C.J. (1996). LISEM: a single-event, physically based hydrological
609 and soil erosion model for drainage basins. I: Theory, input and output. *Hydrological Processes*, **10**:
610 1107-1117.

611 Deng J., Ran J., Wang Z., Fan Z., Wang G., Ji M., Liu J., Wang Y., Liu J., Brown J.H. (2012). Models and
612 tests of optimal density and maximal yield for crop plants. *PNAS*, **109(39)**:15823-15828.

613 Duley F.L. (1939). Surface factors affecting the rate of intake of water by soils. *Soil Science Society of*
614 *America Proceedings*, **4**:60-64.

615 Eghbal M.K., Hajabbasi M.A., Golsefidi H.T. (1996). Mechanism of crust formation on a soil in central
616 Iran. *Plant and Soil*, **180(1)**:67-73.

617 Eldrige D.J., Zaady E., Shachak M. (2000). Infiltration through three contrasting biological soil crusts
618 in patterned landscapes in the Negev, Israel. *Catena*, **40(3)**:323-336.

619 Eurostat (2019). Production of main cereals, EU-27, 2009-2019.
620 [https://ec.europa.eu/eurostat/statistics-](https://ec.europa.eu/eurostat/statistics-explained/index.php?title=File:Production_of_main_cereals,_EU-27,_2009-2019_(million_tonnes)_AFF2020.png)
621 [explained/index.php?title=File:Production_of_main_cereals,_EU-27,_2009-](https://ec.europa.eu/eurostat/statistics-explained/index.php?title=File:Production_of_main_cereals,_EU-27,_2009-2019_(million_tonnes)_AFF2020.png)
622 [2019_\(million_tonnes\)_AFF2020.png](https://ec.europa.eu/eurostat/statistics-explained/index.php?title=File:Production_of_main_cereals,_EU-27,_2009-2019_(million_tonnes)_AFF2020.png). Last access: 24th March 2022.

623 Evrard, O., Biélers, C.L., Vandaele, K., van Wesemael, B. (2007). Spatial and temporal variation of
624 muddy floods in central Belgium, off-site impacts and potential control measures. *Catena*, **70**:443-454.

625 Evrard, O., Vandaele, K., Biélers, C., Wesemael, B. (2008). Seasonal evolution of runoff generation on
626 agricultural land in the Belgian loess belt and implications for muddy flood triggering. *Earth Surface*
627 *Processes and Landforms*, **33**:1285-1301.

628 Evrard O., Cerdan O., van Wesemael B., Chauvet M., Le Bissonnais Y., Raclot D., Vandaele K., Andrieux
629 P., Biélers C. (2009). Reliability of an expert-based runoff and erosion model: Application of STREAM
630 to different environments. *Catena*, **78(2)**:129-141.

631 Evrard, O., Heitz, C., Liégeois, M., Boardman, J., Vandaele, K., Auzet, A.V., van Wesemael, B. (2010). A
632 comparison of management approaches to control muddy floods in central Belgium, northern France
633 and southern England. *Land Degradation & Development*, **21**:322-335.

634 Foley J.L., Loch R.J., Glanville S.F., Connolly R.D. (1991). Effects of tillage, stubble and rainfall energy on
635 infiltration. *Soil and Tillage Research*, **20(1)**:45-55.

636 Garen D.C., Moore D.S. (2005). Curve number hydrology in water quality modeling: Uses, abuses and
637 future directions. *Journal of the American Water Resources Association*, **41(2)**:377-388.

638 Gascuel-Odoux C., Aurousseau P., Cordier M.O., Durand P., Garcia F., Masson V., Salmon-Monviola J.,
 639 Tortrat F., Trepos R. (2009). A decision-oriented model to evaluate the effect of land use and
 640 agricultural management on herbicide contamination in stream water. *Environmental Modelling and*
 641 *Software*, **24**:1433-1446.

642 Gascuel-Odoux C., Aurousseau P., Doray T., Squvidant H., Macary F., Uny D., Grimaldi C. (2011).
 643 Incorporating landscape features to obtain an object-oriented landscape drainage network
 644 representing the connectivity of surface flow pathways over rural catchments. *Hydrological Processes*,
 645 **25**:3625-3636.

646 Gilley J.E., Kottwitz E.R., Wieman G. (1991). Roughness Coefficients for Selected Residue Materials.
 647 *Journal of Irrigation and Drainage Engineering*, **117**:503–514.

648 Grangeon T., Ceriani V., Evrard O., Grison A., Vandromme R., Gaillot A., Cerdan O., Salvador-Blanes S.
 649 (2021). Quantifying hydro-sedimentary transfers in a lowland tile-drained agricultural catchment.
 650 *Catena*, **198**:105033.

651 Gumiere S.J., Raclot D., Cheviron B., Davy G., Louchart X., Fabre J.C., Moussa R., Le Bissonnais Y. (2011).
 652 MHYDAS-Erosion: a distributed single-storm water erosion model for agricultural catchments.
 653 *Hydrological Processes*, **25**:1717-1728.

654 Hawkins R.H. (2014). Curve number method: Time to think anew ? *Journal of Hydrologic Engineering*,
 655 **19**(6). DOI: 10.1061/(ASCE)HE.1943-5584.0000954.

656 Joannon A. (2004). Spatial coordination of cropping systems to control ecological processes. Case study
 657 of runoff in agricultural catchment basins of the Pays de Caux, France. PhD Thesis, 393 pp. INAPG
 658 (AgroParisTech). NNT :2004INAP0018. Pastel-00001257.

659 King, D., Le Bissonnais, Y., (1992). Rôle des sols et des pratiques culturales dans l'infiltration et
 660 l'écoulement des eaux. Exemple du ruissellement et de l'érosion sur les plateaux limoneux du nord de
 661 l'Europe. *Comptes Rendus de l'Academie d'Agriculture de France*, **78**(6): 91–105.

662 King K.W., Arnold J.G., Bingner R.I. (1999). Comparison of Green-Ampt and curve number methods on
 663 Goodwin Creek watershed using SWAT. *Transaction of the ASAE*, **42(4)**:919-925.

664 Le Bissonnais Y., Singer M.J. (1992). Crusting, runoff, and erosion response to soil-water content and
 665 successive rainfalls. *Soil Science Society of America Journal*, **56(6)**:1898-1903.

666 Le Bissonnais Y., Benkhadra H., Chaplot V., Fox D., King D., Daroussin J. (1998). Crusting, runoff and
 667 sheet erosion on silty loamy soils at various scales and upscaling from m² to small catchments. *Soil &*
 668 *Tillage Research*, **46**:69-80.

669 Le Bissonnais Y., Cerdan O., Lecomte V., Benkhadra H., Souchère V., Martin P. (2005). Variability of soil
 670 surface characteristics influencing runoff and interrill erosion. *Catena*, **62**: 111–124.

671 Ludwig B. (1992). L'érosion par ruissellement concentre des terres cultivées du nord du bassin parisien
 672 : analyse de la variabilité des symptômes d'érosion à l'échelle du bassin versant élémentaire. PhD
 673 Thesis, *University of Strasbourg*, 201 pp.

674 Martin P. (1997). Pratiques culturales, ruissellement et érosion diffuse sur les plateau limoneux du
 675 nord ouest de l'Europe. Application aux intercultures du Pays de Caux. PhD Thesis, *INA-PG*, 261 pp.

676 Martin P., Joannon A., Souchère V., Papy F. (2004). Management of soil surface characteristics for soil
 677 and water conservation : The case of a silty loam region (Pays de Caux, France). *Earth Surface Processes*
 678 *and Landforms*, **29**:1105-1115.

679 Martin P., Ouvry J.F., Bockstaller C. (2009). Application of the curve number approach to runoff
 680 estimation for loamy soils over a growing season for winter wheat: Comparison with the STREAM
 681 approach. *Land Degradation and Development*, **21**:376-387.

682 Martin P., Joannon A., Piskiewicz N. (2010). Temporal variability of surface runoff due to cropping
 683 systems in cultivated catchment areas: Use of the DIAR model for the assessment of environmental
 684 public policies in the Pays de Caux (France). *Journal of Environmental Management*, **91**:869-878.

685 Mehdi B., Ludwig R., Lehner B. (2015). Evaluating the impacts of climate change and crop land use
 686 change on streamflow, nitrated and phosphorous: A modeling study in Bavaria. *Journal of Hydrology:*
 687 *Regional Studies*, **4**:60-90.

688 Morgan R.P.C. (2005). Soil erosion and conservation. Third edition, Blackwell Publishing.

689 Moss A.J., Watson C.L. (1991). Rain-impacted soil crust. 3. Effects of continuous and flawed crusts on
 690 infiltration, and the ability of plant covers to maintain crustal flaws. *Australian Journal of Soil Research*,
 691 **29(2)**:311-330.

692 Msigwa A., Chawanda C.J., Komakech H.C., Nkwasa A., Van Griensven A. (under review) Representation
 693 of seasonal land-use dynamics in SWAT+ for improved assessment of blue and green water
 694 consumption. *Hydrology and Earth Systems Sciences*. [https://hess.copernicus.org/preprints/hess-](https://hess.copernicus.org/preprints/hess-2021-171/)
 695 [2021-171/](https://hess.copernicus.org/preprints/hess-2021-171/). Last access: 24th March 2022.

696 Ndiaye B., Esteves M., Vandervaere J.P., Lapetite J.M., Vauclin M. (2005). Effect of rainfall and tillage
 697 direction on the evolution of surface crusts, soil hydraulic properties and runoff generation for a sandy
 698 loam soil. *Journal of Hydrology*, **307**:294-311.

699 Nkwasa A., Chawanda C.J., Msigwa A., Komakech H.C., Verbeiren B., Van Griensven A. (2020). How can
 700 we represent seasonal land use dynamics in SWAT and SWAT+ models for African cultivated
 701 catchments? *Water*, **12**,1541. DOI: 10.3390/w12061541.

702 Osunbitan J.A., Oyedele D.J., Adekalu K.O. (2005). Tillage effects on bulk density, hydraulic conductivity
 703 and strength of a loamy sand soil in southwestern Nigeria. *Soil and Tillage Research*, **82(1)**:57-64.

704 Ouvry J.F., Ligneau L. (1993). A specific strategy set-up with farmers to succeed erosion control – The
 705 experience of a French region Pays de Caux. In: Wicherek S., *Farm land erosion in temperate plains*
 706 *environments and hills*, pp. 497-502.

707 Owens P.N., Batalla R.J., Collins A.J., Gomez B., Hicks D.M., Horowitz A.J., Kondolf G.M., Marden
 708 M., Page M.J., Peacock D.H., Petticrew E.L., Salomons W., Trustrum N.A. (2005). Fine-

709 grained sediment in river systems: environmental significance and management issues. *River*
710 *research and applications*, **21**: 693–717.

711 Peñuela A., Sellami H., Smith H.G. (2018). A model for catchment soil erosion management in humid
712 agricultural environments. *Earth Surface Processes and Landforms*, **43**:608-622.

713 Ponce V.M., Hawkins R.H. (1996). Runoff curve number: has it reached maturity? *Journal of Hydrologic*
714 *Engineering*, **1(1)**:11-19.

715 QGIS (2022). QGIS Geographic Information System. QGIS Association. <http://www.qgis.org>

716 Qi J., Lee S., Zhang X. Yang Q., Mc Carty G.W., Moglen G.E. (2020). Effects of surface runoff and
717 infiltration partition methods on hydrological modeling: A comparison of four schemes in two
718 watersheds in the Northeastern US. *Journal of Hydrology*, **581**:124415.

719 Richet J.B., Ouvry J.F., Pak L.T. (2021) Quantification des ruissellements pour les petits bassins versants
720 limoneux et karstiques de Normandie. Société Hydrotechnique de France, 35-49. ISBN 979-10-93567-
721 24-2. Available at: [https://bassinversant.org/wp-content/uploads/2021/02/Actes-](https://bassinversant.org/wp-content/uploads/2021/02/Actes-ruissellement_compressed.pdf)
722 [ruissellement_compressed.pdf](https://bassinversant.org/wp-content/uploads/2021/02/Actes-ruissellement_compressed.pdf). Last access: 24th March 2022.

723 Saffarpour S., Western A., Adams R., McDonnell J.J. (2016). Multiple runoff processes and multiple
724 thresholds control agricultural runoff generation. *Hydrology and Earth System Sciences*, **20**:4525-4545.

725 Schönhart M., Schmid E., Schneider U.A. (2011). CropRota – A crop rotation model to support
726 integrated land use assessments. *European Journal of Agronomy*, **34**:263-277.

727 Seginer I., Morin J. (1969). The effect of drop impact on the infiltration capacity of bare soils. Israel
728 Institute of Technology, Department of Agricultural Engineering, Publication No. 62. 16p.

729 Shore M., Murphy P.N.C., Jordan P., Mellander P.E., Kelly-Quinn M., Cushen M., Mechan S., Shine O.,
730 Melland A.R. (2013). Evaluation of a surface hydrological connectivity index in agricultural catchments.
731 *Environmental Modelling and Software*, **47**:7-15.

732 Sietz D., Conradt T., Krysanova V., Hatterman F.F., Wechsung F. (2021). The Crop Generator:
 733 Implementing crop rotations to effectively advance eco-hydrological modelling. *Agricultural Systems*,
 734 2021:103183. DOI: 10.1016/j.agsy.2021.103183.

735 Strudley M.W., Green T.R., Ascough II J.C. (2008). Tillage effects on soil hydraulic properties in space
 736 and time: State of the science. *Soil and Tillage Research*, **99**:4-48.

737 Tang X., Song N., Chen Z., Wang J., He J. (2018). Estimating the potential yield and ET_c of winter wheat
 738 across Huang-Huai-Hai Plain in the future with the modified DSSAT model, *Scientific Reports*, **8**:15370.

739 Valentin C. (1991). Surface crusting in two alluvial soils of northern Niger, *Geoderma*, **48**:201-222.

740 Van Dijk P.M., Kwaad F.J.P.M. (1996). Runoff generation and soil erosion in small agricultural
 741 catchments with loess-derived soils. *Hydrological Processes*, **10(8)**:1049-1059.

742 Vinci A., Todisco F., Vergni L., Torri D. (2020). A comparative evaluation of random roughness indices
 743 by rainfall simulator and photogrammetry. *Catena*, **188**:104468.

744 Wagner P.D., Bhallamudi S.M., Narasimhan B., Kumar S., Fohrer N., Fiener P. (2019). Comparing the
 745 effects of dynamic versus static representation of land use change in hydrologic impacts assessments.
 746 *Environmental Modelling and Software*, **122**:103987.